LORI, A NEW RECOMBINANT RNase INHIBITOR FOR *IN VITRO* APPLICATIONS

Sukhov DA[1,2,3], Kholoshenko IV[1,4], Petrova TV[1], Romanenko GA[1,2], Myshkin MYu[3], Kost VYu[3], Trofimov DYu[1], Usman NYu[5] ✉, Barsova EV[3,5]

[1] DNA-Technology LLC, 117587, Moscow, Russia

[2] MIREA — Russian Technological University, Moscow, Russia

[3] Shemyakin-Ovchinnikov Institute of Bioorganic Chemistry RAS, Moscow, Russia

[4] Bauman Moscow State Technical University, Moscow, Russia

[5] Pirogov Russian National Research Medical University, Moscow, Russia

The novel ribonuclease inhibitor LoRI is a 63 kDa recombinant protein optimized for high-throughput expression in *E. coli* and purification by metal chelate affinity chromatography (IMAC). The product was obtained by N-terminal fusion of mouse placental RNase inhibitor polypeptide to a thioredoxin module. Advantage of the engineering strategy in terms of protein structure and function was predicted in silico. Under laboratory settings, the yield of purified soluble recombinant product was about 12 mg per 1 L of expression bacterial culture. By RNase inhibition capacity *in vitro*, the product is comparable or superior to a commercial reference. The kinetic data comply with Lineweaver-Burk model.

Keywords: ribonuclease inhibitor, thioredoxin, immobilized metal chelate affinity chromatography, Lineweaver–Burk model

Funding: The study was funded by DNA-Technology LLC.

Author contribution: Sukhov DA, Romanenko GA — protein engineering, expression and purification; Kholoshenko IV, Petrova TV — product characterization, writing; Myshkin MYu — protein structure analysis; Kost VYu — study design; Trofimov DYu — project supervision; Usman NYu — writing; Barsova EV — project coordination, writing.

✉ **Correspondence should be addressed:** Natalia Yu. Usman
Ostrovityanova 1/1, Moscow, 117997, Russia; n_usman@rambler.ru

Received: 02.09.2024 **Accepted:** 09.10.2024 **Published online:** 28.10.2024

DOI: 10.24075/brsmu.2024.043

НОВЫЙ РЕКОМБИНАНТНЫЙ ИНГИБИТОР РНКаз LORI ДЛЯ ПРИМЕНЕНИЯ *IN VITRO*

Д. А. Сухов[1,2,3], И. В. Холошенко[1,4], Т. В. Петрова[1], Г. А. Романенко[1,2], М. Ю. Мышкин[3], В. Ю. Кост[3], Д. Ю. Трофимов[1], Н. Ю. Усман[5] ✉, Е. В. Барсова[3,5]

[1] ООО «ДНК-Технология», Москва, Россия

[2] МИРЭА — Российский технологический университет, Москва, Россия

[3] Институт биоорганической химии имени М. М. Шемякина и Ю. А. Овчинникова, Москва, Россия

[4] Московский государственный технический университет имени Н. Э. Баумана, Москва, Россия

[5] Российский национальный исследовательский медицинский университет имени Н. И. Пирогова, Москва, Россия

Ингибиторы РНКазы давно используют в биотехнологии и лабораторной диагностике. Целью работы было получить и охарактеризовать новый рекомбинантный ингибитор РНКаз LoRI. Полученный новый ингибитор рибонуклеаз LoRI представляет собой рекомбинантный белок массой 63 кДа, оптимизированный для высокопроизводительной экспрессии в *E. coli* и очистки с помощью металлохелатной аффинной хроматографии (IMAC). Продукт получен за счет *N*-концевого слияния полипептидной последовательности плацентарного ингибитора РНКаз мыши с тиоредоксиновым модулем. Целесообразность данной модификации с точки зрения структуры и функции белка подтверждена *in silico*. Выход очищенного растворимого рекомбинантного продукта в лабораторных условиях составил около 12 мг на 1 л экспрессионной бактериальной культуры. По активности *in vitro* продукт сопоставим с коммерческим аналогом или превосходит его. Кинетические данные соответствуют модели Лайнуивера–Берка.

Ключевые слова: ингибитор рибонуклеаз, тиоредоксин, металлохелатная аффинная хроматография (IMAC), модель Лайнуивера–Берка

Финансирование: исследование выполнено при финансовой поддержке ООО «ДНК-Технология».

Вклад авторов: Д. А. Сухов, Г. А. Романенко — инженерия, экспрессия и очистка белков; И. В. Холошенко, Т. В. Петрова — характеризация продукта, написание статьи; М. Ю. Мышкин — анализ структуры белка; В. Ю. Кост — дизайн исследования; Д. Ю. Трофимов — руководство проектом; Н. Ю. Усман — написание статьи; Е. В. Барсова — координация проекта, написание статьи.

✉ **Для корреспонденции:** Наталья Юрьевна Усман
ул. Островитянова, д. 1/1, г. Москва, 117997, Россия; n_usman@rambler.ru

Статья получена: 02.09.2024 **Статья принята к печати:** 09.10.2024 **Опубликована онлайн:** 28.10.2024

DOI: 10.24075/vrgmu.2024.043

Specific proteins that directly inhibit cellular and extracellular ribonucleases (RNases) are expressed by various cell types and their overall physiological effect is cytoprotective [1]. Kinetic studies on RNase inhibition by these proteins used several model targets, notably RNase A and angiogenin — a secreted RNase with low catalytic activity, promoting vascularization [2]. Experiments with angiogenin and placental RNase inhibitor revealed a two-step binding mechanism, with rapidly formed loose complex of the two proteins E·I eventually tightened into stable E·I* complex by slow isomerization (k_2 = 97 s^{-1}) [3].

RNase inhibitors have long been used in biotechnology and laboratory diagnostics. The highly efficient RNase inhibition is essential for the accuracy of reverse transcription-based analytical methods, as underscored by the diagnostic experience during SARS-CoV2 pandemic [4]. Large-scale production of recombinant RNase inhibitors in bacterial systems is complicated due to redox sensitivity of these proteins [5] which may also impair their stability at storage.

Thioredoxins (Trx), small proteins found in all living cells, participate in redox control, which involves the electron retention capacity of cysteine residues in the active site of Trx. By sponging the electron flux from NADPH (catalyzed by Trx reductase) Trx stabilize activated thiolate groups in miscellaneous cellular proteins thereby protecting their

native, active state [6]. In protein engineering, the use of Trx as a covalently linked chaperone can substantively improve the yields of a redox-sensitive recombinant product without compromising its properties; the overall benefit will depend on details of both the expression system and the target product. In *E. coli*-based systems, a Trx fusion module may effectively prevent the product from being misfolded and sequestered to inclusion bodies. *E. coli* Trx transcripts are highly translated in authentic media thus supporting high yields of the chimeric protein; in addition, Trx has a robust tertiary structure and can be further modified for metal chelate purification [7].

This article describes production and characterization of a novel recombinant RNase inhibitor LoRI, constructed from the mouse placental RNase inhibitor polypeptide, supplemented with a thioredoxin module to enhance redox stability and a His tag for advanced purification by metal affinity chromatography (IMAC).

METHODS

Protein engineering

Murine ribonuclease inhibitor sequence retrieved from UniProt database (*M. musculus* Rnh1; Uniprot Q91VI7) was fused at the N-terminus to thioredoxin module (*E. coli* trxA; Uniprot P0AA25) via a linker comprising hexahistidine tag (6H), thrombin recognition site (LVPRGS), S-Tag (KETAAAKFERQH), and enterokinase recognition site (DDDDK):

MNHKVHMNSDKIIHLTDDSFDTDVLKADGAILVDFWAEWC
GPCKMIAPILDEIADEYQGKLTVAKLNIDQNPGTAPKYGIRGIPT
LLLFKNGEVAATKVGALSKGQLKEFLDANLAGSGSGHMHHH
HHHSSGLVPRGSGMKETAAAKFERQHMDSPDLGTDDDDKA
MSLDIQCEQLSDARWTELLPLIQQYEVVRLDDCGLTEVRCKDI
SSAVQANPALTELSLRTNELGDGGVGLVLQGLQNPTCKIQKLS
LQNCGLTEAGCGILPGMLRSLSTLRELHLNDNPMGDAGLKLL
CEGLQDPQCRLEKLQLEYCNLTATSCEPLASVLRVKADFKELV
LSNNDLHEPGVRILCQGLKDSACQLESLKLENCGITAANCKDL
CDVVASKASLQELDLSSNKLGNAGIAALCPGLLLPSCKLRTLW
LWECDITAEGCKDLCRVLRAKQSLKELSLASNELKDEGARLLC
ESLLEPGCQLESLWIKTCSLTAASCPYFCSVLTKSRSLLELQMS
SNPLGDEGVQELCKALSQPDTVLRELWLGDCDVTNSGCSSL
ANVLLANRSLRELDLSNNCMGGPGVLQLLESLKQPSCTLQQL
VLYDIYWTNEVEEQLRALEEERPSLRIIS*

In silico study used the AlphaFold 3 protein structure prediction model [8].

Molecular cloning and bacterial expression system

Codon optimization for *E. coli* was based on codon usage data retrieved from public sources (NCBI GenBank, Codon Usage Database). The nucleotide sequence was further adjusted manually to minimize the prevalence of GC-rich regions while preserving the encoded amino acid identity. De novo synthesis of the nucleotide sequence by assembly with partially overlapping oligonucleotides and subsequent amplification was ordered as a service from Evrogen JSC (Moscow, Russia) and performed according to original protocol by Dr. A. F. Fradkov in 2021.

The codon-optimized trxA-6H-Rnh1 DNA template was cloned into pET32 plasmid (Pharmacia). The construct was verified by Sanger sequencing. To potentiate expression of the active recombinant protein in *E. coli* system, electrocompetent *E. coli* BL21(DE3) (Novagen) were transformed with pGro7 chaperone plasmid (Takara Bio) to enable GroEL-ES assisted folding advisable for cysteine-rich recombinant products [9]. The obtained producer strain *E. coli* BL21(DE3)-pGro7 was transformed with the pET32-trxA-6H-Rnh1 construct.

Bacterial culture

The *BL21(DE3)-pGro7* producer strain transformed with the pET32-trxA-6H-Rnh1 expression plasmid was grown overnight at 37 °C in LB broth containing 10 g/L NaCl, 10 g/L tryptone and 5 g/L yeast extract, with ampicillin and chloramphenicol added to final concentrations of 100 μg/mL and 30 μg/mL, respectively. The culture was subsequently re-inoculated to a fresh flask with antibiotic-supplemented LB and incubated overnight at 37 °C/225 rpm. Next day, the pre-culture was diluted in LB supplemented with 2.5 mM $MgCl_2$ and grown in a F25L bioreactor (BioTechno Group; Russia) at 37 °C, 400 rpm, 0.6 bar and 0.25 m^3/h to exponential phase defined as OD_{600} = 0.5. At this point, the culture was induced with 1 g/L arabinose to activate the chaperone genes and allowed to grow at 37 °C to OD_{600} = 0.9. The temperature was subsequently reduced to 20 °C and the culture was induced with isopropyl β-d-1-thiogalactopyranoside (IPTG) at a final concentration of 1 mM. Twenty hours post-induction the cells were collected at 4,500 rpm in a Beckman Coulter Avanti™ J-15R centrifuge equipped with Beckman Coulter Avanti™ JS-4.750 rotor (Beckman Coulter; USA).

Protein extraction

A 50 g total yield of bacterial cells expressing Trx-RI fusion protein was resuspended in 10 v/v of Ni-A buffer solution (500 mM NaCl, 20 mM Tris-Cl, 10 mM Imidazole (ImH), 0.1% Tween 20, 10 mM 2-mercaptoethanol (2-bme); pH 7.6) with 1 mM PMSF and lysed with Q500 ultrasonic homogenizer (Qsonica, USA) set at amplitude 60, pulse on/off 05/05 s for 10 min on ice. The lysate was clarified by centrifugation in HERMLE Z-36HK equipped with HERMLE 12/035 rotor (HERMLE Labortechnik GmbH, Germany) at 21,000 rpm for 40 min. To precipitate soluble proteins, the clarified lysate was supplemented with 15% w/w $(NH_4)_2SO_4$ and centrifuged in HERMLE Z-36HK with HERMLE 12/035 rotor at 21,000 rpm for 10 min, then supplemented with 10% w/w $(NH_4)_2SO_4$ and centrifuged identically. The supernatant was discarded and the pellet was dissolved in 5 v/v of Ni-A. The purified protein solution was passed through a 0.22 μm polyethersulfone filter membrane (Vacuum Filtration „rapid"-Filtermax; TPP, Switzerland).

Chromatography

The filtered product was loaded onto an XK 26/20 chromatography column (Cytiva, USA) filled with Ni-INDIGO resin (Cube Biotech GmbH; Germany). The column volume (CV, 20 mL) was pre-equilibrated with 15 CV of Ni-A buffer at a rate of 5 mL/min. The loading proceeded at a rate of 4 mL/min. The loaded column was washed with 10 CV of Ni-A buffer. The elution used 5 CV of 0.5X Ni-B buffer and 5 CV of 1X Ni-B buffer (500 mM NaCl, 20 mM Tris-Cl, 500 mM ImH, 0.1% Tween 20, 10 mM 2-bme; pH 7.6) (Fig. 1).

The eluate was analyzed by 10% SDS–PAGE (Figure 2). Fractions containing the recombinant target product were pooled and dialyzed in Q-A buffer (20 mM Tris-Cl, 120 mM KCl, 0.1 % Tween 20, 10 mM 2-bme; pH 7.2) at 1:40 v/v for 12 h.

High-performance anion exchange chromatography II used a HiScale™ 16/10 column filled with Q Sepharose Fast Flow (CV=10 mL; Cytiva) pre-equilibrated with 15 CV of Q-A buffer.

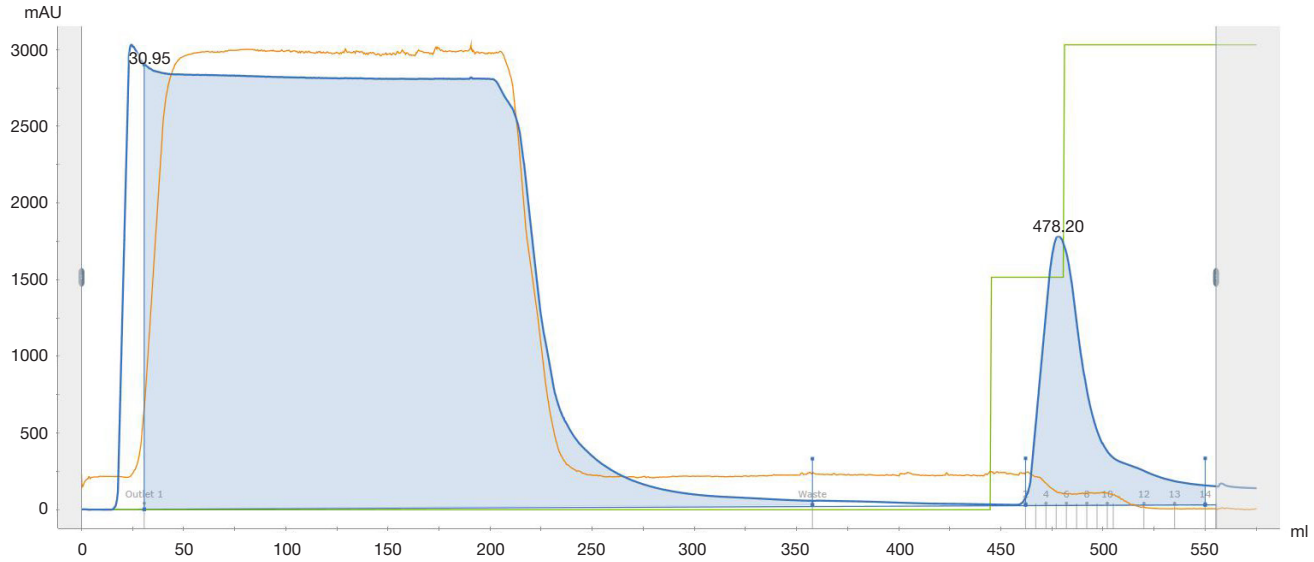

Fig. 1. Chromatography I profile (IMAC on Ni-INDIGO, Cube Biotech)

The filtered dialysate was loaded onto the column at a rate of 3 mL/min (Supplementary Fig. S1). The loaded column was washed with 10 CV of Q-A buffer. The elution used 20 CV of 0–15% Q-B buffer (20 mM Tris-Cl, 1 M KCl, 0.1% Tween 20, 10 mM 2-bme; pH 7.2).

Fractions of interest containing the recombinant product were determined by SDS–PAGE (7–26; Supplementary Fig. S2), pooled and dialyzed in storage buffer (50 mM KCl, 20 mM Hepes-K, 0.1 % Tween 20, 8 mM DTT, 50% Glycerol; pH 7.2) at 1:40 v/v for 12 h. After dialysis, concentration and purity of the product were assessed by spectrophotometry using Bradford method and by SDS–PAGE with bovine serum albumin as a standard (Supplementary Fig. S3). The stock was diluted to 1 mg/mL (15.75 μM) with storage buffer (pH = 7.0), aliquoted and stored at –25…–18 °C.

Commercial reference

Thermo Scientific™ RiboLock RNase Inhibitor 40 U/μL (#EO0381) was chosen as RNasin activity reference. Molecular weight of the protein, 49.6 kDa, was provided in the manufacturer's data. Concentration of the protein in supplied aliquots, 1 mg/mL (20.16 μM), was determined using Bradford method.

RNA substrates

Two types of RNA prep were used as substrates: (1) human total RNA isolated from HEK 293 cell cultures using ExtractRNA reagent (Evrogen; Russia); and (2) synthetic single-stranded RNA, 1.7 kb, obtained by transcription in vitro using HiScribe T7 High Yield RNA Synthesis Kit (NEB #E2040S). RNA concentrations were measured in NanoDrop™ 2000/2000c at 260/280 and 260/230 absorbance ratios; the integrity was verified by electrophoresis.

RNA stability assay

The ribonuclease inhibitor (RNasin) activity was assessed through extent of RNA degradation in the presence of RNase A.

Monarch® RNase A 20 mg/mL (NEB #T3018L) was selected as a model partner for the inhibitory binding. Working solution of the target was obtained by dilution of the stock with pure deionized water to 5 ng/μL. The RNase inhibition activity is

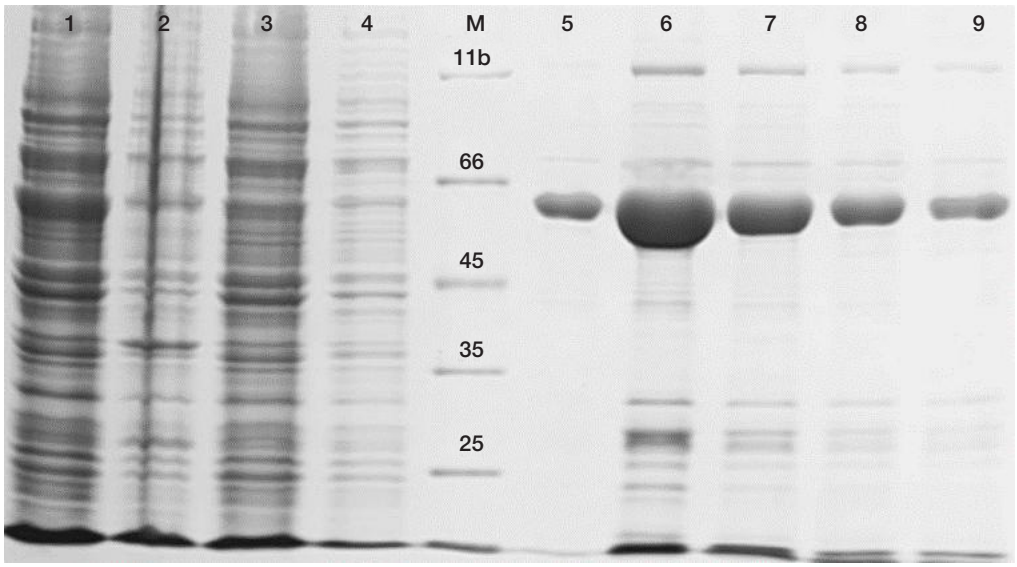

Fig. 2. Chromatography I samples, 10% SDS–PAGE. Lanes: 1 — supernatant; 2 — insoluble residue; 3 — flow-through; 4 — wash; M — protein molecular weight marker with band values, kDa, indicated in the image; 5–9 — eluted fractions 2, 5, 8, 10 and 11, respectively

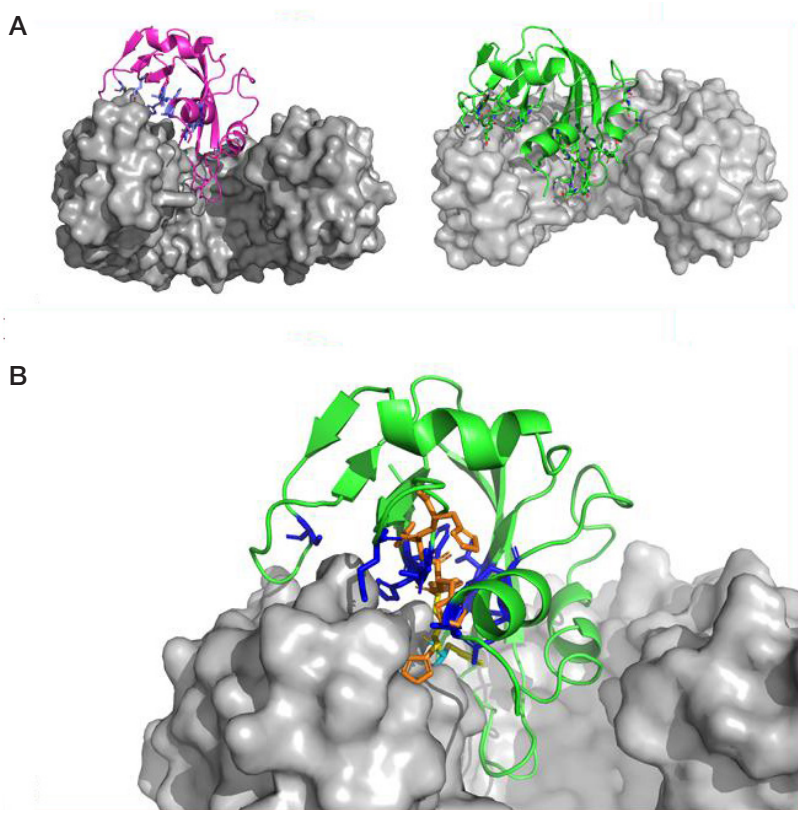

Fig. 3. Ribonuclease A (RibA) interacts with core inhibitor Rnh1 (grey surface). **A**. The enzyme contacts the inhibitor with its ligand-binding groove; the residues forming the active center are highlighted (PDB id: 1DFJ) [10]. **B**. Enlarged image of the C-terminus in close contact with residues of the active site in ribonuclease (blue) which sterically hinders the RNA binding. The histidine tag at the C-terminus (orange) disrupts the interaction by 'protruding' into RibA; overlay of AlphaFold3 model of Rnh1 with C-terminal His tag and crystal structure of Rnh1/RibA complex (PDB id: 1DFJ).

conventionally measured in units, with single unit corresponding to the amount of agent capable of reducing the activity of 5 ng of RNase A to 50% of initial value.

The reactions were set up in buffer (10 mM TrisHCl, 2 mM $MgCl_2$, 10 mM KCl, pH 8.0 at 25 °C) with 0.3–1.0 μg human total RNA, 2.5–5.0 ng RNase A and 0.0–4.0 μg inhibitor (LoRI or RiboLock). The inhibitor and the RNase were premixed and added to RNA. The 10 μL reaction mixtures were incubated under varying conditions, basically at 37 °C for 30 min, and analyzed by 1.2% agarose gel electrophoresis. The RNase A reaction was terminated by addition of 2-bme to 0.5 M and the mixtures were placed on ice or frozen. Before electrophoresis, the samples were mixed with gel loading buffer (#PB020; Evrogen). For reverse transcription, the aliquots were sampled before the addition of 2-bme and analyzed immediately.

Fluorimetry

The RNA stability was monitored by fluorimetry with Ribo488 RNA Quantification Reagent (product code 11510, Lumiprobe, Russia). Kinetic curves of RNA degradation were built using CLARIOstar® Plus microplate reader (BMG LABTECH, Germany) in AMC enzyme kinetics mode.

Specific activity assay used Lumiprobe QuDye ssDNA Reagent (product code 17102, Lumiprobe) with synthetic single-stranded RNA combined to 2.5 ng RNase A and 0.5–4.0 μg inhibitor in 40 μL reaction volume. The binding proceeded at 37 °C for 1 hour. The measurements were made in a Hidex Sense 425-311 microplate reader (HIDEX; Finland).

Kinetic study used human total RNA and Lumiprobe QuDye ssDNA Reagent. The mixtures were set up using 10X Reaction Buffer (300 mM TrisHCl, 50 mM $MgCl_2$, 500 mM KCl; pH 7.9-8.0 at 25 °C) with varying amounts of RNA (150, 300, 600 ng) and LoRI (1, 0.9, 0.8 μg — respectively, 197, 177, 157 nM in 80 μL reaction volume); the measurements were made in CLARIOstar® Plus. The reference Thermo Fisher™ RiboLock inhibitor was used in a final concentration of 252 nM. RNase A (5 ng per reaction) was used as a target; the RNase-free and inhibitor-free controls were included in the series, representing the intact substrate and the uninhibited enzymatic degradation samples, respectively.

PCR tests

RNA quantification by reverse transcription PCR used OneTube RT-PCR TaqMan setup (# SK031; Evrogen, Russia) with primers flanking a 130 bp fragment of *B2M* cDNA (5'-ATTATAACCCTA CATTTTGTG, 5'-TGTAAGCAGCATCATGGAGGTT, 0.2 μM each) and a TaqMan probe covering exon junction to exclude noise from residual genomic DNA (5'-FAM-GCCGCATTTGGATTGGATGAATTCCA-BHQ1, 0.1 μM).

PCR (non)inhibition tests used 5X qPCRmix-HS PCR setup (# PK145; Evrogen) with a FAM-BHQ1 TaqMan system. A 90 bp fragment of *GAPDH* was amplified from 100 pg of human genomic DNA in 25 μL reaction volume. All tests were run in 5 technical replicates in a BioRad CFX 96 real-time amplification instrument (BioRad; USA).

RESULTS

In silico structural study

The prototypical ribonuclease inhibitor Rnh1 has multiple leucine-rich repeat motifs and its overall folded shape resembles a horseshoe lined with negatively charged residues. Fig. 3A shows Rnh1 binding ribonuclease A (RibA), a small

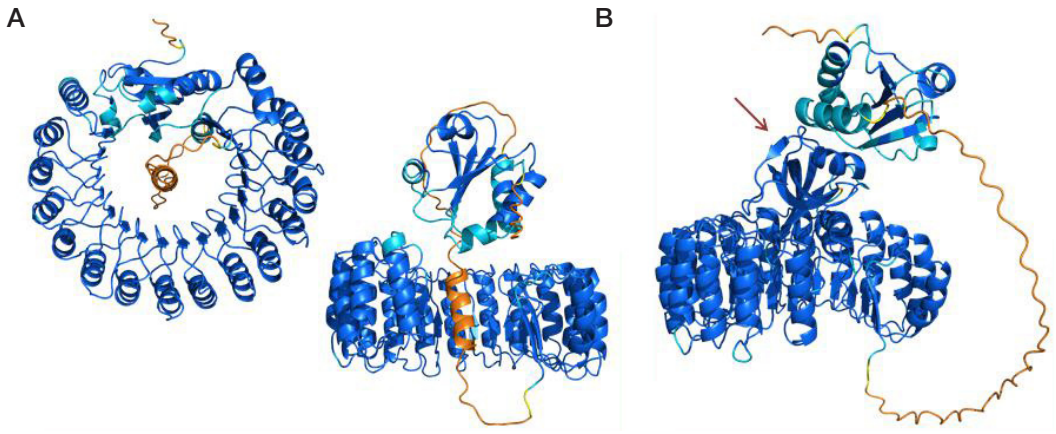

Fig. 4. AlphaFold3 models of Trx::Rnh1 fusion product. **A**. The product, native and unbound, comprising the horseshoe-shaped core inhibitor connected via linker to the compact Trx. The color scheme reflects predicted local distance difference test (pLDDT), a per-residue model confidence score provided by AlphaFold3, with pLDDT > 90, *blue*, high-confidence model; pLDDT 70–90, *light-blue*, high confidence for the backbone; pLDDT 50–70, *yellow* (low-confidence representation of a volatile structure); and pLDDT < 50, *orange*, region unstructured in isolation. Accordingly, the Rnh1 and Trx functional modules are imaged with high accuracy, whereas representation of the linker is conditional: it can be oriented and located differently e.g. outside the horseshoe. **B**. RibA (*arrow*) appears sandwiched between Trx and Rnh1 modules of the fusion product

protein of ~120 amino acids stabilized by four disulfide bonds. The binding involves C-terminal region of the inhibitor, notably positions V405, V428, Y430, D431, Y433 and E436 [10]. The inhibition mechanism is based on steric hindrance of the active site in RibA. Importantly, N-terminal region of the inhibitor does not participate in the interaction, which makes it a preferable location for a fusion point (especially since fusing Trx at the C-terminus would have excluded it as a cis chaperone module that should be already in place by the time of Rnh1 synthesis). Moreover, a His tag at the C-terminus was predicted to interfere with the ligand binding (Fig. 3B) which ultimately determined the engineering strategy.

Fig. 4A shows the Trx::Rnh1 fusion protein, with two compact functional modules of high prediction accuracy connected by loose, disordered linker. AlphaFold3 images of the Trx::Rnh1/RibA complex show close juxtaposition of Trx and RibA moieties during the interaction (Fig. 4B).

Thus, Trx module may stabilize the complex by 'pressing' RibA to the inhibitor. Electrostatically, the 'pressure' is favored by a negative surface potential on Trx. The estimated total charge of Trx module is –4, whereas the ribonuclease molecule has a total charge of +4 and electrostatically positive surface (to attract RNA) apart from a single cluster of negatively charged residues. In addition, Trx may act as an enzyme itself, opening the exposed disulfides in RibA and thereby disrupting its structure while bound to the inhibitor (Supplementary Fig. S4).

Yields

The design afforded a 3–5-fold increase in yields of soluble recombinant protein compared with unmodified Rnh1 sequence. The raw yields were estimated 2.7–3 mg of recombinant target per 1 g of E. coli biomass. The cumulative losses at all purification steps amounted to 25–30%. The yield

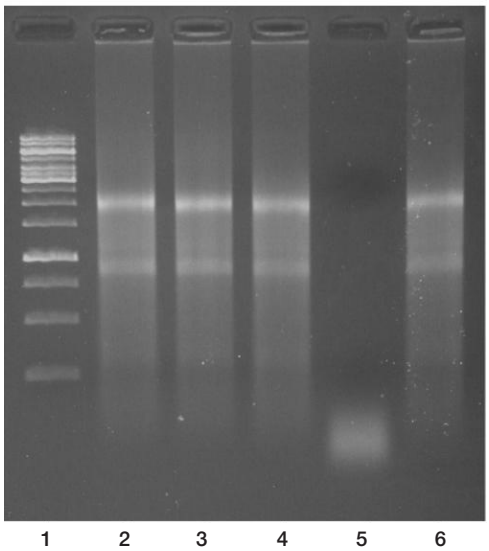

	2	3	4	5	6
RNase A	–	–	5 ng	5 ng	5 ng
LoRI		1 µg	1 µg	–	–
Thermo Scientific™ RiboLock	–	–	–	–	1 µg

Fig. 5. RNA stability assay, pilot series. Lane 1: Thermo Scientific™ GeneRuler 1kb DNA Ladder. Lanes 2–6: 1 µg RNA +. The treatment proceeded at 37 °C for 30 min.

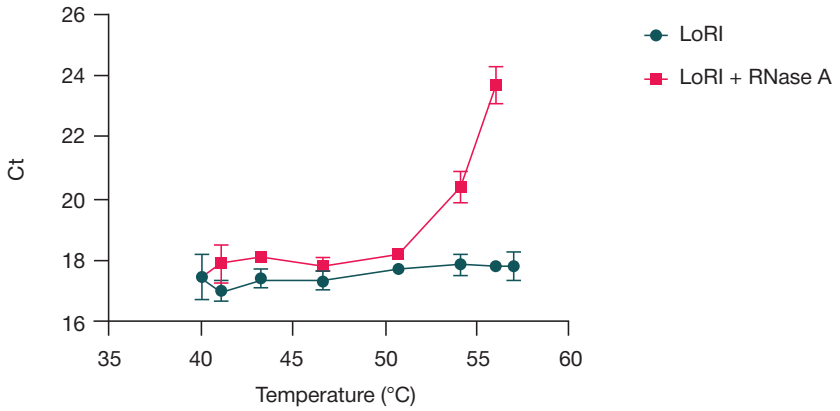

Fig. 6. Reverse transcription PCR data for RNA stability assay at 40–57 °C using 1 µg RNA + 2 µg LoRI with or without RNase A (2.5 ng), treatment time — 30 min

of purified active product under laboratory conditions was 2 mg per 1 g of *E. coli* biomass, or about 12 mg per 1 L of expression culture.

RNA stability assay

Pilot tests using 1 µg of human total RNA combined to 5 ng RNase A and 1 µg LoRI in 10 µL reaction volume revealed excellent protective properties of the product towards RNA (Fig. 5).

The effective temperature range of inhibition was determined using a 40–57 °C temperature gradient programmed in a thermal block. The setup used 1 µg of human total RNA combined to 2.5 ng RNase A and 2 µg LoRI in 10 µL reaction volume. For comparison, identical samples of total RNA + LoRI were incubated for 30 minutes at the same range of fixed temperatures without added RNase. The 30 min incubations were followed by collection of 1 µL aliquots for PCR tests of RNA integrity run immediately; the data are shown in Fig. 6. The remaining portions were 2-bme-treated and analyzed by electrophoresis (Fig. 7, Supplementary Fig. S5).

Alternative setups varying the reaction parameters are shown in Supplementary Figs. S6–S14. The data show that LoRI fully preserves RNA at temperatures up to 46.6 °C with further increase leading to partial RNA degradation. At 54.1 °C electropherograms show a diffuse smear shifted to a low-molecular-weight region (Fig. 7, lane 4), while Ct increases by 3 cycles corresponding to a one-order decrease in effective concentration of the 130 b template (Fig. 6). At 57.0 °C, the protective properties of LoRI are residual: electropherograms shows full degradation of the sample with ΔCt reaching 7 cycles compared with the initial value.

PCR (non)inhibition tests

The data indicate no change in PCR efficiency in the presence of up to 4.0 µg of LoRI in a 25 µl reaction volume (Supplementary Fig. S15).

Specific activity assay

Calibration curve for the assay is shown in Supplementary Fig. S16. Considering the linear response range of 0.1–0.6 µg, all measurements were performed with 1.0 µg RNA in order to improve the inhibition kinetics plot accuracy against Thermo Fisher™ RiboLock RNase Inhibitor (40 U/µL ~ 1 µg/µL) as a reference activity. Fluorescence measurements for excess of an inhibitor were accepted as 100%. Based on the data, 1 µg of LoRI was found to correspond to 50 U (Supplementary Fig. S17).

Comparative kinetic study

The Lineweaver-Burk graphical model assuming a mixed ribonuclease inhibition mechanism is shown in Supplementary Fig. S18.

The inhibition constant value, Ki, determined by the graphical representation approach was consistent with computational

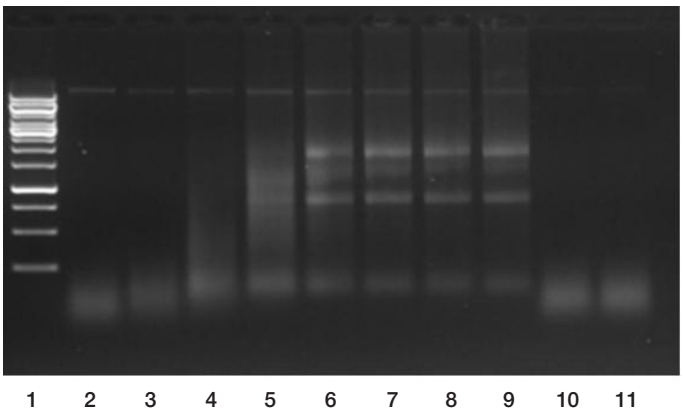

Fig. 7. RNA stability assay at 40–57 °C, treatment time— 30 min. Lane 1: Thermo Scientific™ GeneRuler 1kb DNA Ladder Lanes 2–9: 1 µg RNA + 2.5 ng RNase A + 2 µg LoRI at

2	3	4	5	6	7	8	9
57.0 °C	56.0 °C	54.1 °C	50.7 °C	46.6 °C	43.3 °C	41.1 °C	40.0 °C

Lanes 10–11: 1 µg RNA + 2.5 ng RNase A, no inhibitor added, incubated at 57.0 and 40.0 °C, respectively.

findings for the mixed inhibition model [11]. The calculated inhibition constant for LoRI towards RNase A constituted 0.825 pM. The approach was further applied to calculate the inhibition constant for Thermo Fisher™ RiboLock, which constituted 1.199 pM. According to the data, LoRI outperformed the reference activity in terms of inhibitory capacity associated with the formation of a low-dissociation enzyme-inhibitor complex.

DISCUSSION

The study was aimed at developing an RNase inhibitor for use in precision molecular medicine, in particular in diagnostic test systems based on reverse transcription PCR and library preparation for RNA sequencing. The proposed strategy of Trx fusion in combination with His-tagging was successful. The product is intended for a wide scope of research and diagnostic applications.

The growing demand for effective RNase inhibitors of molecular biological quality is related to the current interest in RNA as a key information carrier in molecular medicine and related medical biotechnology; the latest products include diagnostic kits, RNA vaccines, etc. The placental RNase inhibitor Rnh1 is an ideal prototype agent for preserving RNA isolated from cell cultures or tissues. A major obstacle to its industrial-scale production is redox-sensitivity: this leucine-rich repeat protein contains about 30 cysteine residues per molecule, all of which must be reduced to form SH groups and prevented from intramolecular disulfide bonding [12]. Overexpression of unmodified Rnh1 in *E. coli* is undermined by foreign redox environment, suboptimal synthesis rates and missing chaperone apparatus. The misfolded recombinant protein tends to irretrievably precipitate in the form of inclusion bodies. Klink et al (2001) overexpressed porcine inhibitor in *E. coli* using *trp* promoter and minimal growth medium to isolate ~10 mg of purified active product per liter of culture; typically for the time, purification used affinity chromatography with immobilized RNase A [13]. Another (historical) alternative was to isolate the inhibitor from fresh animal tissues; the approach yielded ~6 mg of inhibitor per kg of wet liver tissue using ribonuclease affinity chromatography followed by anion-exchange chromatography, and a similar amount from the placenta [14]. In modern realities, the RNase affinity chromatography is disadvantageous in terms of versatility and costs, especially concerning the risks of downstream trace contamination with RNase.

CONCLUSIONS

The use of Trx module as intramolecular chaperone in bacterial expression system afforded high yields of the mammalian prototype-based recombinant ribonuclease inhibitor in soluble active form after purification by IMAC. The product shows excellent RNA preservation properties under a broad range of conditions relevant to molecular research and laboratory diagnostics.

References

1. Thomas SP, Kim E, Kim JS, Raines RT. Knockout of the ribonuclease inhibitorgGene leaves human cells vulnerable to secretory ribonucleases. Biochemistry. 2016; 55 (46): 6359–62. DOI: 10.1021/acs.biochem.6b01003.
2. Abel RL, Haigis MC, Park C, Raines RT. Fluorescence assay for the binding of ribonuclease A to the ribonuclease inhibitor protein. Anal Biochem. 2002; 306 (1): 100–07. DOI: 10.1006/abio.2002.5678.
3. Lee FS, Shapiro R, Vallee BL. Tight-binding inhibition of angiogenin and ribonuclease A by placental ribonuclease inhibitor [published correction appears in Biochemistry 1989 Mar 7; 28 (5): 2354]. Biochemistry. 1989; 28 (1): 225–30. DOI: 10.1021/bi00427a031.
4. Nishibata Y, Koshimoto S, Ogaki K, Ishikawa E, Wada K, Yoshinari M, Ishizu A. RNase in the saliva can affect the detection of severe acute respiratory syndrome coronavirus 2 by real-time one-step polymerase chain reaction using saliva samples. Pathol Res Pract. 2021; 220: 153381. DOI: 10.1016/j.prp.2021.153381.
5. Šiurkus J, Neubauer P. Heterologous production of active ribonuclease inhibitor in Escherichia coli by redox state control and chaperonin coexpression. Microb Cell Fact. 2011; 10: 65. DOI: 10.1186/1475-2859-10-65.
6. Lee S, Kim SM, Lee RT. Thioredoxin and thioredoxin target proteins: from molecular mechanisms to functional significance. Antioxid Redox Signal. 2013; 18 (10): 1165–207. DOI: 10.1089/ars.2011.4322.
7. LaVallie ER, Lu Z, Diblasio-Smith EA, Collins-Racie LA, McCoy JM. Thioredoxin as a fusion partner for production of soluble recombinant proteins in Escherichia coli. Methods Enzymol. 2000; 326: 322–40. DOI: 10.1016/s0076-6879(00)26063-1.
8. Abramson J, Adler J, Dunger J, et al. Accurate structure prediction of biomolecular interactions with AlphaFold 3. Nature. 2024; 630: 493–500 DOI: 10.1038/s41586-024-07487-w.
9. Kyratsous CA, Silverstein SJ, DeLong CR, Panagiotidis CA. Chaperone-fusion expression plasmid vectors for improved solubility of recombinant proteins in Escherichia coli. Gene. 2009; 440 (1–2): 9–15. DOI: 10.1016/j.gene.2009.03.011.
10. Kobe B, Deisenhofer J. A structural basis of the interactions between leucine-rich repeats and protein ligands. Nature. 1995; 374 (6518): 183–6. DOI: 10.1038/374183a0.
11. Dixon M, Webb EC. Enzymes. 2nd Edition. New York: Academic Press, 1964.
12. Fominaya JM, Hofsteenge J. Inactivation of ribonuclease inhibitor by thiol-disulfide exchange. J Biol Chem. 1992; 267 (34): 24655–60.
13. Klink TA, Vicentini AM, Hofsteenge J, Raines RT. High-level soluble production and characterization of porcine ribonuclease inhibitor. Protein Expr Purif. 2001; 22 (2): 174–9. DOI: 10.1006/prep.2001.1422.
14. Dickson KA, Haigis MC, Raines RT. Ribonuclease inhibitor: structure and function. Prog Nucleic Acid Res Mol Biol. 2005; 80: 349–74. DOI: 10.1016/S0079-6603(05)80009-1.

Литература

1. Thomas SP, Kim E, Kim JS, Raines RT. Knockout of the ribonuclease inhibitorgGene leaves human cells vulnerable to secretory ribonucleases. Biochemistry. 2016; 55 (46): 6359–62. DOI: 10.1021/acs.biochem.6b01003.
2. Abel RL, Haigis MC, Park C, Raines RT. Fluorescence assay for the binding of ribonuclease A to the ribonuclease inhibitor protein. Anal Biochem. 2002; 306 (1): 100–07. DOI: 10.1006/abio.2002.5678.
3. Lee FS, Shapiro R, Vallee BL. Tight-binding inhibition of angiogenin and ribonuclease A by placental ribonuclease inhibitor [published correction appears in Biochemistry 1989 Mar 7; 28 (5): 2354]. Biochemistry. 1989; 28 (1): 225–30. DOI: 10.1021/bi00427a031.
4. Nishibata Y, Koshimoto S, Ogaki K, Ishikawa E, Wada K, Yoshinari M, Ishizu A. RNase in the saliva can affect the detection of severe acute respiratory syndrome coronavirus 2 by real-time one-step

polymerase chain reaction using saliva samples. Pathol Res Pract. 2021; 220: 153381. DOI: 10.1016/j.prp.2021.153381.
5. Šiurkus J, Neubauer P. Heterologous production of active ribonuclease inhibitor in Escherichia coli by redox state control and chaperonin coexpression. Microb Cell Fact. 2011; 10: 65. DOI: 10.1186/1475-2859-10-65.
6. Lee S, Kim SM, Lee RT. Thioredoxin and thioredoxin target proteins: from molecular mechanisms to functional significance. Antioxid Redox Signal. 2013; 18 (10): 1165–207. DOI: 10.1089/ars.2011.4322.
7. LaVallie ER, Lu Z, Diblasio-Smith EA, Collins-Racie LA, McCoy JM. Thioredoxin as a fusion partner for production of soluble recombinant proteins in Escherichia coli. Methods Enzymol. 2000; 326: 322–40. DOI: 10.1016/s0076-6879(00)26063-1.
8. Abramson J, Adler J, Dunger J, et al. Accurate structure prediction of biomolecular interactions with AlphaFold 3. Nature. 2024; 630: 493–500 DOI: 10.1038/s41586-024-07487-w.
9. Kyratsous CA, Silverstein SJ, DeLong CR, Panagiotidis CA. Chaperone-fusion expression plasmid vectors for improved solubility of recombinant proteins in Escherichia coli. Gene. 2009; 440 (1–2): 9–15. DOI: 10.1016/j.gene.2009.03.011.
10. Kobe B, Deisenhofer J. A structural basis of the interactions between leucine-rich repeats and protein ligands. Nature. 1995; 374 (6518): 183–6. DOI: 10.1038/374183a0.
11. Dixon M, Webb EC. Enzymes. 2nd Edition. New York: Academic Press, 1964.
12. Fominaya JM, Hofsteenge J. Inactivation of ribonuclease inhibitor by thiol-disulfide exchange. J Biol Chem. 1992; 267 (34): 24655–60.
13. Klink TA, Vicentini AM, Hofsteenge J, Raines RT. High-level soluble production and characterization of porcine ribonuclease inhibitor. Protein Expr Purif. 2001; 22 (2): 174–9. DOI: 10.1006/prep.2001.1422.
14. Dickson KA, Haigis MC, Raines RT. Ribonuclease inhibitor: structure and function. Prog Nucleic Acid Res Mol Biol. 2005; 80: 349–74. DOI: 10.1016/S0079-6603(05)80009-1.